

ADMM-MCBF-LCA: A Layered Control Architecture for Safe Real-Time Navigation

Anusha Srikanthan*, Yifan Xue*, Vijay Kumar, Nikolai Matni, Nadia Figueroa

Abstract—We consider the problem of safe real-time navigation of a robot in a dynamic environment with moving obstacles of arbitrary smooth geometries and input saturation constraints. We assume that the robot detects and models nearby obstacle boundaries with a short-range sensor and that this detection is error-free. This problem presents three main challenges: i) input constraints, ii) safety, and iii) real-time computation. To tackle all three challenges, we present a layered control architecture (LCA) consisting of an offline path library generation layer, and an online path selection and safety layer. To overcome the limitations of reactive methods, our offline path library consists of feasible controllers, feedback gains, and reference trajectories. To handle computational burden and safety, we solve online path selection and generate safe inputs that run at 100 Hz. Through simulations on Gazebo and Fetch hardware in an indoor environment, we evaluate our approach against baselines that are layered, end-to-end, or reactive. Our experiments demonstrate that among all algorithms, only our proposed LCA is able to complete tasks such as reaching a goal, safely. When comparing metrics such as safety, input error, and success rate, we show that our approach generates safe and feasible inputs throughout the robot execution.

I. INTRODUCTION

Historically, motion planning algorithms [1] decouple the planning problem from feedback control design. The challenge today is to integrate these approaches to ensure safe robot behavior. To this end, layered control architectures (LCAs) offer a design methodology for robot navigation using hierarchical layers balancing constraint complexity and trajectory horizons: see the recent survey [2] which highlights the success of LCAs across robotics and other application areas. Many works [2]–[5] employ LCAs where higher layers solve model predictive control (MPC) over long horizons at low frequencies, while lower layers handle trajectory tracking at higher frequencies. However, integrating these layers is challenging due to mismatched time scales, real-time computational requirements, and task completion objectives. Real-time solutions [6], [7] often rely on offline libraries of reference trajectories or reachable sets, combined with online planning, but these components assume partial or complete knowledge of the environment and can be difficult to coordinate effectively. In contrast, we assume that obstacles within a local radius are visible to the robot, and aim to ensure safety through reactive control.

*-Equal Contribution

We gratefully acknowledge the support of NSF Grant CCR-2112665, NSF awards CPS-2038873, SLES-2331880, AFOSR Award FA9550-24-1-0102 and NSF CAREER award ECCS-2045834. for this research.

A. Srikanthan, Y. Xue, V. Kumar, N. Matni, and N. Figueroa are with the School of Engineering and Applied Science, University of Pennsylvania, Philadelphia, USA (e-mail: {sanusha, yifanxue, kumar, nmatni, nadiafig}@seas.upenn.edu).



(a) Safe Real-Time Navigation

(b) RVIZ visualization

Fig. 1: We show a Fetch robot successfully reaching a goal in a dynamic environment running our proposed algorithm to avoid a human walking around and other static obstacles. Blue and green shades in Figure 1b are obstacles, while the green trajectories are ADMM-generated feasible paths.

Although reactive control strategies for safety-critical robot navigation [8], such as artificial potential fields [9], navigation functions [10], [11], dynamical system (DS) based modulation [12], [13] and control barrier functions (CBFs) [14]–[16], are computationally effective; they are limited by their greedy policies for long-horizon planning for control-affine input-constrained systems. Such policies struggle to escape local minima (saddle points) in cluttered non-convex environments that are not ball [15] or star worlds [17] resulting in sub-optimal trajectories and failed mission objectives. Further, designing reactive control strategies for nonholonomic vehicles, such as differential drive robots, adds the challenge of contradicting input and safety constraints alongside the use of simplified dynamics models [18]. Reactive methods largely rely on a nominal global trajectory encoding task objectives for mission completion. Unlike planning methods that design reference trajectories, we generate path libraries consisting of nominal controllers, feedback gain matrices and reference trajectories. This allows us to relax input constraints at the reactive layer, as we will show, drastically reducing solver infeasibility that plague reactive controllers.

Therefore, in this paper, we offer an LCA that generates an offline library of feasible paths for control-affine input-constrained systems while allowing for smooth transitions between paths with an online path selector that tracks the closest global trajectory with a reactive control strategy ensuring safety in real-time. While one could use any of the aforementioned reactive control strategies, in our proposed LCA framework, we choose the recently introduced on-manifold Modulated CBF method (MCBF) [19]. The MCBF method applies the notion of on-manifold navigation, initially formulated for DS modulation [20], to the CBF safety

filter framework eliminating local minima for any arbitrarily shaped obstacle.

Our contributions are as follows.

- 1) To achieve real-time performance while ensuring task completion (e.g., reaching a goal), we propose a layered solution that consists of offline path generation and an online safety filter, as shown in Figure 2.
- 2) Using the generated library of feasible controllers, feedback gain matrices, and reference trajectories satisfying state constraints, we construct a nominal feedback law that is easy to track for reactive controllers while also ensuring smooth transitions between paths.
- 3) With online path selection and a MCBF safety filter that eliminates local minima, we ensure safety in cluttered environments with arbitrarily shaped static and dynamic obstacles. Our online execution layer runs at 100 Hz.
- 4) We provide an open-source implementation of our approach and baselines¹.

In Section II, we discuss prior work from related topics to contextualize our contributions, and introduce the problem in Section III. In Section IV, we propose our layered framework as shown in Figure 2 consisting of an offline library generation layer and an online execution layer. In Section V, we show comparisons of our method against baselines, highlighting the benefits of layering and long-horizon multi-path offline libraries. We end with concluding remarks in Section VI.

II. RELATED WORK

We discuss related work on two degree of freedom (2DOF) architectures and LCAs to motivate the use of the alternating direction method of multipliers (ADMM) algorithm for path generation. We also provide an overview of reactive methods for obstacle avoidance to motivate the use of MCBF.

A. 2DOF and Layered Control Architectures

In linear control systems, the term 2DOF controllers refer to control laws that consist of a feedforward term, which drives the system to the desired trajectory, and a feedback term to compensate for errors [21]. Analogous design patterns are observed in robust MPC. For example, tube-based MPC approaches broadly apply a control input of the form $u = K(x - x_d) + u_d$, where (x_d, u_d) are nominal state and control inputs computed by solving an optimization problem online, and $K(x - x_d)$ is a feedback term compensating for errors between the actual system state x and the reference state x_d . For nonlinear systems, trajectory generation and feedback control are typically decoupled, although approaches exist that do not explicitly make this separation, e.g., iLQR [22]. In this paper, we exploit the structure of ADMM applied to optimal control problems (OCP) [23] to obtain a 2DOF controller with a feedforward term and feedback gains. We use the time-varying feedback gain matrices online to locally stabilize the system whenever

the robot switches from one path to the next due to the presence of an obstacle.

B. Reactive methods for Obstacle Avoidance

Collision-free guarantees in dynamic environments are achieved either through the satisfaction of constraints in optimization-based approaches [14], [24]–[28] or through reactive potential-field inspired closed-form solutions [9], [12], [29]–[34]. Among all methods, only CBF-QP [14] can minimize deviations from nominal controller behavior while ensuring safety for general control-affine systems and a general class of obstacle geometries [35]. While methods to enforce robot input constraints optimally for Dynamical System motion policy modulation (Mod-DS) are proposed in [19], its applications are limited to fully actuated systems. Although variants of CBF-QP, such as CBF-CLF-QP are available for safe reactive navigation tasks without the use of a nominal controller, designing the Control Lyapunov Function (CLF) for navigation tasks in general is challenging and not the focus of this work. In this paper, we generate feasible paths offline to alleviate the need for enforcing tight input constraints online and guide the robot to the goal while maintaining safety through reactive methods.

III. BACKGROUND AND PROBLEM FORMULATION

Consider a continuous-time control-affine nonlinear system of the form

$$\dot{x}(t) = f(x(t)) + g(x(t))u(t) \quad (1)$$

where $t, t_f \in \mathbb{R}$ are continuous-time parameters with t ranging from 0 to t_f , $x(t) \in \mathbb{R}^n$ is a state vector, $u(t) \in \mathbb{R}^m$ is a control input vector, and $f: \mathbb{R}^n \rightarrow \mathbb{R}^n$, and $g: \mathbb{R}^n \rightarrow \mathbb{R}^{n \times m}$ define the control-affine nonlinear dynamics. Our objective is to design $u(t)$ to bring the system (1) from initial state $x(0) = \xi$ to goal state $x(t_f) = \xi_g$ while remaining safe and satisfying input constraints, i.e., $u(t) \in \mathcal{U}$ where

$$\mathcal{U} = \{u \in \mathbb{R}^m \mid u_{\min} \leq u \leq u_{\max}\}. \quad (2)$$

We define the notion of robot safety and consider safe control algorithms based on boundary functions. Given a twice-differentiable function h_j for each obstacle $j \in \mathcal{O}_{x,t}$ where $\mathcal{O}_{x,t}$ denotes the set of visible obstacle indices, we define a safe set with boundary function $h_j: \mathbb{R}^n \times \mathbb{R}^p \rightarrow \mathbb{R}$ as the following,

$$\mathcal{C} = \{x \in \mathbb{R}^n \mid h_j(x, x_o^j(t)) > 0, \forall j \in \mathcal{O}_{x,t}, t \in [0, t_f]\}, \quad (3)$$

where x_o^j is the instantaneous obstacle state including its position and orientation and p is the obstacle state dimension.

Given the above definitions, we formulate an optimal control problem (OCP) with an objective function J as

$$\begin{aligned} & \text{minimize} && \int_0^{t_f} J(x(t), u(t)) \\ & \text{subject to} && \dot{x}(t) = f(x(t)) + g(x(t))u(t), \quad t \geq 0, \\ & && u(t) \in \mathcal{U}, \quad t \geq 0, \\ & && x(t) \in \mathcal{C}, \end{aligned} \quad (4)$$

while satisfying boundary conditions given by $x(0) = \xi$ and $x(t_f) = \xi_g$. The problem in (4) poses three challenges: a)

¹https://github.com/yifanxueseas/admm_mcbf_lca

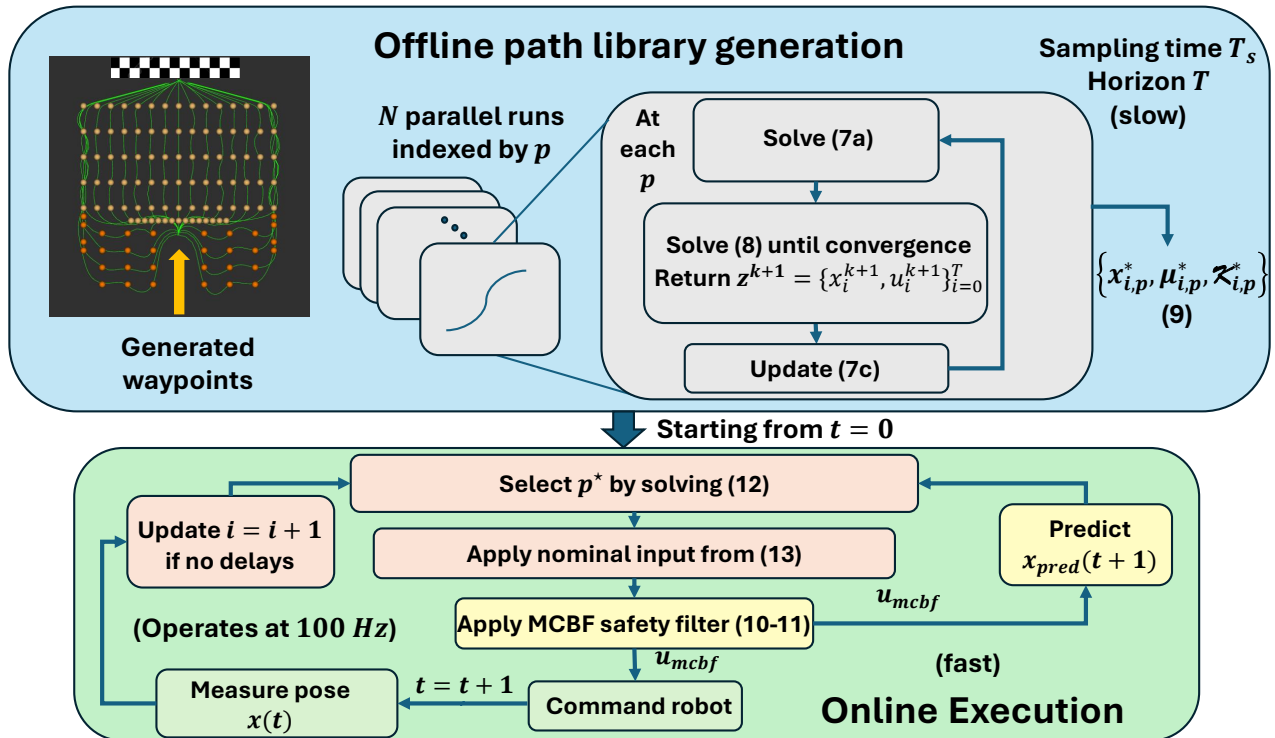


Fig. 2: We present a schematic of our approach showing the offline path library generation on the top in blue and online execution in green. We generate a total of N nominal controllers by using a fixed set of waypoints to sufficiently cover the initial known safe set. When commanding the robot, we use nearest neighbor search over predicted next states to choose a path where ties are broken by choosing the one closer to the center. We construct our nominal feedback input and apply a safety filter using an on-Manifold control barrier function. Finally, this is applied to the robot in real-time.

input constraint satisfaction, b) safety, and c) real-time computation. To handle safety and real-time computation, prior work [10], [11], [14] design reactive controllers to maintain the state within a time-invariant safe set. Recent work [24], [36] tackles input constraint satisfaction and safety by using MPC to solve a discrete-time version of (4). In practice, nonlinear MPC suffers from computational burden and solver infeasibility for long-horizon problems. Several works [4], [5] attempt to tackle all three challenges through LCAs running low-frequency MPC without safety constraints at the higher layer and CBF-QP at the lower layer. However, without careful coordination between the layers, we empirically observe that such approaches i) still suffer from local minima in cluttered environments with concave obstacles and ii) may lead to infeasible solutions for control-affine systems with tight input constraints ($u(t) \in \mathcal{U}$).

Problem Statement: To address the combined problem of input feasibility, safety and real-time computation in (4), we consider the design of offline long-horizon path planners, accompanied by fast online feedback solvers and an appropriate reactive strategy to ensure safety and task completion.

IV. ADMM-MCBF AS A LAYERED CONTROL ARCHITECTURE

Our goal is to design a long-horizon path planner to guide the system to a goal state, while leveraging reactive policies to ensure safety. To this end, we propose a layered solution that consists of an offline path planner used to generate a feasible path library, an online path selector, and an online

safety filter as shown in Figure 2. The feasible path library provides controllers, reference trajectories, and time-varying feedback gain matrices to stabilize the system locally around the generated trajectories. Moreover, these gains allow for a smooth proportional control action whenever the robot transitions between paths if the robot is near an obstacle.

A. Offline Feasible Path Library Generation

1) *Waypoint generation:* The trajectories associated with each path in the path library are regulated by two user-design choices: the inter-trajectory intervals δ , and the number of waypoints per trajectory τ . We assume that the users have access to the approximate size of the exploration field, i.e., how large an area the robot explores to complete a task (e.g., reaching a goal). For example, given a room of width L , we generate $N = L/\delta$ offline paths. We choose δ sufficiently small to provide the robot with the flexibility to avoid getting trapped. For most of the scenarios we consider, we grid sample a fixed number of points along the direction towards the goal dispersed by δ (colored yellow in Figure 2). In other scenarios where trajectories evolve away from the goal, we sample points (colored in orange in Figure 2) by selecting some of them manually to improve optimization convergence of the algorithm in the following section.

2) *Nominal Controller Design:* To design N input feasible feedback controllers such that their resulting trajectories satisfy the generated waypoints, we consider a discrete-time nonlinear system obtained by the Runge-Kutta discretization

of (1) with a sampling time of T_s seconds as

$$x_{i+1} = f_d(x_i, u_i) \quad (5)$$

where f_d is the discretized dynamics, $x_i \in \mathbb{R}^n$ is a state vector and $u_i \in \mathbb{R}^m$ is a control input vector at discrete time step i . Our objective is to design discrete-time feedback controllers over a finite horizon T such that the input satisfies saturation constraints given by $u_i \in \mathcal{U}$. We do not consider safety constraints in this design step.

Let $T/(\tau+1) = \Delta$ such that Δ is divisible by T_s and the time indices at which waypoint constraints are enforced be $\mathcal{T} = \{\Delta, 2\Delta, \dots, \tau\Delta\}$. The problem is succinctly described as the following constrained OCP solved for each nominal controller indexed by p as

$$\begin{aligned} & \text{minimize} && \sum_{i=0}^{T-1} J_i(x_{i,p}, u_{i,p}) \\ & \text{subject to} && x_{i+1,p} = f_d(x_{i,p}, u_{i,p}), u_{i,p} \in \mathcal{U}, i \geq 0, \\ & && x_{0,p} = \xi, x_T = \xi_g, \\ & && x_{i,p} = w_p(\lfloor i/\Delta \rfloor), \forall i \in \mathcal{T}, \end{aligned} \quad (6)$$

where J_i are stage costs, and $w_p(\cdot)$ enumerates the generated waypoints for controller p . To solve problem (6), we introduce redundant state and input equality constraints as in [23] and apply the ADMM algorithm. To simplify notation, we drop references to indices p and describe our algorithm for a single nominal controller. We note that computing the N nominal controllers can be easily parallelized.

For each nominal controller, define a state trajectory variable as \mathbf{x} , input trajectory variable as \mathbf{u} , and the combined trajectory variable as $\mathbf{z} = (\mathbf{x}^\top, \mathbf{u}^\top)^\top$. We introduce a redundant trajectory variable $\bar{\mathbf{z}}$ and an equality constraint $\mathbf{z} = \bar{\mathbf{z}}$ to optimization in (6). Let $\mathbf{J}(\bar{\mathbf{z}}) = \sum_{i=0}^{T-1} J_i(\bar{\mathbf{z}}_i)$, $\psi(\mathbf{z}; \xi) = \sum_{i=0}^{T-1} \psi(z_i, \xi)$ be a sum of indicator functions for dynamics constraints given as

$$\psi(z_i; \xi) = \begin{cases} 0, & \text{if } x_{i+1,p} = f_d(x_{i,p}, u_{i,p}), \forall i > 0 \\ 0, & \text{if } x_{0,p} = \xi, i = 0 \\ \infty, & \text{otherwise,} \end{cases}$$

and $\bar{\psi}(\bar{\mathbf{z}}; w_p) = \sum_{i=0}^{T-1} \bar{\psi}(\bar{\mathbf{z}}_i; w_p)$ be the sum of indicator functions for waypoints and input constraints defined as

$$\bar{\psi}(\bar{\mathbf{z}}_i; w_p) = \begin{cases} 0, & \text{if } i \in \mathcal{T}, \bar{z}_{u,i} \in \mathcal{U}, \text{ and } \bar{z}_{x,i} = w_p(i/\Delta), \\ 0, & \text{if } i \notin \mathcal{T}, \bar{z}_{u,i} \in \mathcal{U}, \bar{z}_{x,T} = \xi_g \\ \infty, & \text{otherwise,} \end{cases}$$

where $\bar{z}_{x,i}$ and $\bar{z}_{u,i}$ correspond to state and input redundant variables at time i , respectively.

To obtain a layered decomposition [23], we apply the ADMM algorithm to (6), yielding the following iterative updates

$$\begin{aligned} \bar{\mathbf{z}}^{k+1} &:= \underset{\bar{\mathbf{z}}}{\operatorname{argmin}} \mathbf{J}(\bar{\mathbf{z}}; \xi_g) + \frac{\rho}{2} \|\mathbf{z}^k - \bar{\mathbf{z}} + \mathbf{v}^k\|_2^2 \\ & \text{s.t. } \bar{\psi}(\bar{\mathbf{z}}; w_p) = 0, \end{aligned} \quad (7a)$$

$$\begin{aligned} \mathbf{z}^{k+1} &:= \underset{\mathbf{z}}{\operatorname{argmin}} \frac{\rho}{2} \|\mathbf{z} - \bar{\mathbf{z}}^{k+1} + \mathbf{v}^k\|_2^2 \\ & \text{s.t. } \psi(\mathbf{z}, \xi) = 0 \end{aligned} \quad (7b)$$

$$\mathbf{v}^{k+1} := \mathbf{v}^k + \mathbf{z}^{k+1} - \bar{\mathbf{z}}^{k+1}, \quad (7c)$$

where $\mathbf{z}, \bar{\mathbf{z}}$ are primal variables, \mathbf{v} is a scaled dual variable and ρ is a tuning parameter to improve convergence of the ADMM algorithm. Moreover (7a) is a time separable feasibility problem without dynamics constraints that can benefit from parallelization, while (7b) is an unconstrained OCP with nonlinear dynamics and a quadratic objective function which can be solved via sequential linearization-based techniques, such as iLQR. Finally, the dual updates in (7c) ensure consistency so as to guarantee both constraint satisfaction and dynamic feasibility at convergence. We note here that one could choose any constrained optimization method to solve (6), however, using the proposed ADMM-based decomposition facilitates computing feedback gain matrices, as discussed below.

If \mathbf{J} is convex, the only nonconvex part of the problem is the *unconstrained* nonlinear dynamics found in the update step (7b). By isolating the nonconvexity of the problem to this update step, we can leverage iLQR [22] to rapidly converge to a locally optimal solution under fairly benign assumptions [37]. In what follows, we show how we solve (7b) using iLQR, resulting in local convergence to an optimal feedback controller that tracks the reference trajectory $\bar{\mathbf{z}}$ from (7a).

3) *Feedback controller from ADMM iterates:* For any ADMM iteration $k+1$, let $\mathbf{d}^k = -(\mathbf{z}^k - \bar{\mathbf{z}}^{k+1} + \mathbf{v}^k)$. By doing a change of variable from \mathbf{x}, \mathbf{u} to $\delta\mathbf{x} = \mathbf{x} - \mathbf{x}^k$ and $\delta\mathbf{u} = \mathbf{u} - \mathbf{u}^k$, and setting $\delta\mathbf{z} = (\delta\mathbf{x}^\top, \delta\mathbf{u}^\top)^\top$, the feedback control problem in (7b) is approximately solved via iLQR:

$$\begin{aligned} \delta\mathbf{z}^{\ell+1} &:= \underset{\delta\mathbf{z}}{\operatorname{argmin}} \frac{\rho}{2} \|\delta\mathbf{z} - \mathbf{d}^\ell\|_2^2 \\ & \text{s.t. } \delta z_{x,i+1} = [A_i^\ell \ B_i^\ell] \delta z_i \end{aligned} \quad (8)$$

where ℓ is iLQR iteration counter and the constraint in (8) is from linearization of the dynamics constraints f_d with $[A_i^\ell \ B_i^\ell] = \frac{\partial f_d(\mathbf{z})}{\partial \mathbf{z}}|_{\mathbf{z}=\mathbf{z}^{k+\ell}}$. Solving (8) using dynamic programming results yields time-varying feedback gain matrices $\mathcal{K}_{i,p}^*$ [22]. Once the ADMM algorithm has converged, for the p th nominal controller at any discrete-time index i we have

$$\mu_{i,p}^*, \mathcal{K}_{i,p}^*, x_{i,p}^* \quad (9)$$

the nominal input, the feedback gain matrices, and the resulting state vector respectively. We report the time taken for convergence of the algorithm with different sampling times (T_s) and trajectory horizons (T) in Table I. We next illustrate how the feedback gain matrices from each nominal controller $\mathcal{K}_{i,p}^*$ play a role in stabilizing the system online whenever the MCBF safety filter modifies the nominal inputs.

B. Online Safe Reactive Control

In this section, we first describe the MCBF controller we solve online using the selected nominal inputs and provide details of our proposed architecture in the green block of Figure 2.

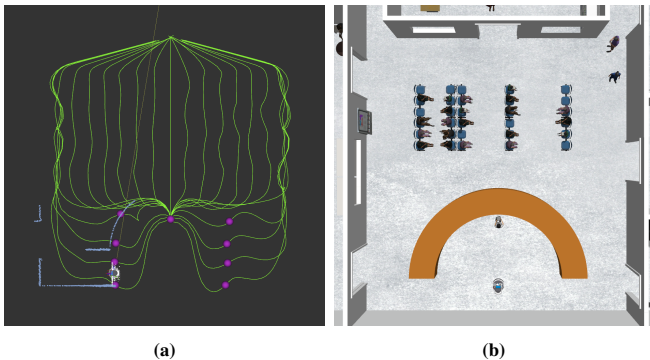


Fig. 3: In 3a, we show the feasible trajectories from our path library in green visualizing the computed offline solutions for the initially unknown environment in 3b. The pink dots indicate the feasible next states to choose from. The nearby detected obstacle boundaries are visualized as blue point clouds.

1) *Reactive Control with MCBF:* While our proposed LCA could use any reactive strategy, to generate safe inputs that ensure no local minima we use the modulation based on-Manifold Modulated CBF-QP (MCBF-QP) [19]. Control inputs synthesized by CBF-QPs inevitably result in saddle points even for fully-actuated robots (see [19, Thm. 5.3]). To eliminate the saddle points of CBF-QP solvers and their variants, MCBF-QP modulates the dynamics and projects components onto the tangent planes of the obstacle boundary functions, introducing tangential velocities. This is achieved by introducing an additional constraint on the standard CBF-QP formulations as in (11). The MCBF-QP is presented below:

$$u_{mcbf} = \operatorname{argmin}_{u \in \mathbb{R}^p} (u - u_{nom})^\top (u - u_{nom})$$

$$L_f h(x, x_o) + L_g h(x, x_o)u + \nabla_{x_o} h(x, x_o) \dot{x}_o \geq -\alpha(h(x, x_o)) \quad (10)$$

$$\phi(x, x_o)^\top f(x) + \phi(x, x_o)^\top g(x)u \geq \gamma, \quad (11)$$

where L_f and L_g are the Lie derivatives of $h(x, x_o)$. Here, γ is the user's choice of a strictly positive real number, and the tangent direction $\phi(x, x_o)$ can be derived using various obstacle exit strategies, such as hessian or geometric approximation. See [19] and [20] for implementation details.

2) *Online Path Selector:* To achieve obstacle avoidance in real-time and ensure task completion, we initialize the path at $t = 0$ using the center-line connecting initial state to the goal. For $t > 0$, we first run a nearest neighbor search algorithm to decide which path to track:

$$p^*(t+1) = \operatorname{argmin}_p \|\{x_{i,p}^*\}_{p=0}^N - x_{pred}(t+1)\|, \quad (12)$$

where $x_{pred}(t+1) = f_d(x(t), u_{mcbf}(t))$ with $u_{mcbf}(t)$ as the optimized input from solving MCBF-QP (IV-B.1). Ties are broken by selecting the one closer to the center-line connecting the initial state to the goal. Once we obtain $p^*(\cdot)$, we construct the nominal input with a feedback term as

$$u_{nom}(t) = \mu_{i,p^*}^* + \mathcal{K}_{i,p^*}^*(x_{i,p^*}^* - x(t)). \quad (13)$$

The feedback control law in (13) has a feedforward term μ_{i,p^*} that drives the robot toward the goal in the absence of

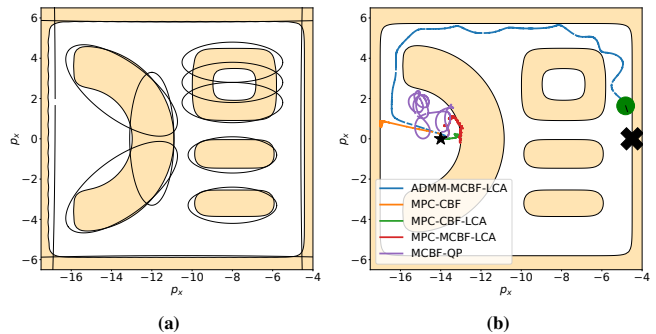


Fig. 4: In 4a, we show boundaries of the obstacle inside hospital Gazebo simulations that are learned using GPDF [38], and the ellipse approximations used by MPC-CBF solver. In 4b, we plot the results from Gazebo simulations of our approach and 4 baselines for the indoor environment with unknown obstacles. We observe that ours shown in blue is the only approach that reaches the goal while ensuring safety.

Horizon (T)	Sampling Time (T_s)	Avg. Time (secs)
16	0.5	2.090
40	0.2	7.545
80	0.1	23.175
160	0.05	47.635
400	0.02	209.595

TABLE I: We report the time taken to compute 5 paths for different values of horizon T and T_s on the unicycle model for 5 randomly sampled initial conditions given the same goal condition. In our GitHub repository, we also provide several other dynamics models to test on.

obstacles. When the robot is near an obstacle, the feedback term \mathcal{K}_{i,p^*}^* is a proportional compensation for deviations from the nearest x_{i,p^*}^* resulting in a smooth transition between paths. We emphasize that these feedback gain matrices \mathcal{K}_{i,p^*}^* are derived from (7), not tuned manually. When no obstacles are present, $u_{mcbf} \approx u_{nom}$, while in obstacle situations, \mathcal{K}_{i,p^*} compensates for the deviations. Our online execution runs at 100 Hz, solving in under 0.01 seconds on average.

V. EXPERIMENTS

In this section, we evaluate our proposed method on the differential drive robot Fetch through realistic Gazebo simulations and qualitative hardware experiments. We compare our proposed ADMM-MCBF-LCA against four baselines, each representing a category of prior work on safe real-time robot navigation in dynamic environments. We use metrics such as input tracking error, solver infeasibility, collision-free rate, and task success. For ADMM, we use the ρ -update rule described in [39, §3.4.1, equation (3.13)] to improve convergence. We provide custom implementations of all algorithms using `cvxpy` [40], CasADi [41] and JAX optimizers [42]. Empirically, we found $\delta = 0.8m$ to be a reasonable interval size for Fetch robot navigation tasks for our dynamic environment settings.

The first baseline is MPC-CBF [24], which solves OCPs with a discrete-time CBF constraint. The second and third baselines use MPC with CBF-QP and MCBF-QP safety filters, similar to prior multirate control works [2]–[5]. We demonstrate that our method complements these approaches, highlighting the advantage of layered solutions for better

Algorithms	QP-solver fail # ↓	Safety % ↑	Task success % ↑	Lin. speed (\bar{v}) ↑	Ang. speed ($\bar{\omega}$) ↓	v err. (e_v) ↓	ω err. (e_ω) ↓
<i>ADMM-MCBF-LCA</i>	0	100	100	0.487	0.584	0.012	0.027
<i>MPC-CBF</i>	-	100	0	0.100	1.303	0.011	0.074
<i>MPC-CBF-LCA</i>	0	100	0	0.048	0.537	0.005	0.024
<i>MPC-MCBF-LCA</i>	33	100	0	0.024	1.246	0.008	0.037
<i>MCBF-QP</i>	19	60	0	0.380	0.989	0.015	0.051
<i>MPPI</i>	-	100	0	0.036	0.312	0.037	0.035

TABLE II: We report the metrics for all algorithms evaluated from 5 gazebo trials showing in bold the metrics for which our proposed ADMM-MCBF-LCA performed the best. We use \uparrow and \downarrow to indicate if higher or lower is better, respectively. \bar{v} and $\bar{\omega}$ are the average linear and angular speeds and their average tracking errors are denoted by $e_{\bar{v}}, e_{\bar{\omega}}$. The first three columns indicate algorithm performance in terms of QP solver failure across trials, % collision-free trials, and % task completion rate.

performance. The final reactive baseline, MCBF-QP [19], is a reactive policy with a naive single integrator model as its nominal controller, underscoring the importance of well-designed nominal controllers. We also provide a comparison with a sampling-based variant of MPC, biased Model Predictive Path Integral (MPPI) [43].

A. Robot Dynamics and Obstacle Definitions

For all experiments, we model Fetch using the unicycle nonlinear dynamics given as

$$\dot{x} = \begin{bmatrix} \dot{p}_x \\ \dot{p}_y \\ \dot{\theta} \end{bmatrix} = \begin{bmatrix} \cos \theta & 0 \\ \sin \theta & 0 \\ 0 & 1 \end{bmatrix} \begin{bmatrix} v \\ \omega \end{bmatrix} \quad (14)$$

where v, ω are the linear and angular speeds such that $v_{max} = 1\text{m/s}$, $\omega_{max} = 2\text{m/s}$, $v_{min} = \omega_{min} = 0$. The state of the robot consists of 2-D Euclidean position p_x, p_y , and orientation θ .

To apply the MCBF-QP and CBF-QP approaches, the CBF must have relative degree 1, i.e., the control input must appear in the first time-derivative of the CBF. Since the control input ω for (14) is of relative degree 2 to the CBFs used, instead of a signed distance function we use a higher-order CBF (HO-CBF) [44], [45] of relative degree 1 with respect to control inputs v, ω . HO-CBF $h_{OH}(x, x_o^j)$, shown in Eq. (15), is defined on robot position and orientation, where $h(p_x, p_y, x_o^j)$ is the robot’s orthonormal distance to the obstacle surface, and w is a scalar weight.

$$h_{OH}(x, x_o^j) = h(p_x, p_y, x_o^j) + w \frac{\partial h(p_x, p_y, x_o^j)}{\partial p_x} \cos \theta + w \frac{\partial h(p_x, p_y, x_o^j)}{\partial p_y} \sin \theta \quad (15)$$

Our experiments highlight how judiciously combining a properly designed global nominal controller with a MCBF-QP filter (based on a HO-CBF) can achieve stable and safe navigation in crowded and concave environments. For all methods except MPC-CBF, the obstacle boundaries are obtained using learned Gaussian Process Distance Fields (GPDF) [38]. Since MPC-CBF requires discrete-time CBF constraints, we instead use ellipse approximations, as shown in Figure 4a. In our approach, the index i is updated based on progress to $x_{i,p}^*$ using distance measurements, adjusting for delays within a user-specified tolerance.

B. Results

The task for the robot is to navigate an indoor hospital environment as shown in Figure 4b starting within the

concave obstacle desk and reach the other end of the room. Among all approaches, only our approach safely navigates the robot to the goal shown in Figure 4b. We summarize metrics in Table II, where $\bar{v}, \bar{\omega}$, are average linear and angular speeds, $e_{\bar{v}}, e_{\bar{\omega}}$ are errors in tracking linear and angular speeds, computed as deviations between commanded and measured inputs. On hardware as shown in Figure 1, we show our robot safely navigating around a human walking in the robot’s exploration space.

From the results reported, we observe that MCBF-QP controller fails to reach the goal although it is guaranteed to escape local minima. We believe that this is due to large model mismatch from using a naive dynamics model for nominal input design. Using discrete-time MPC with CBF constraints (MPC-CBF) struggles with navigating Fetch out of concave obstacles due to large tracking errors from low update frequencies. The nonlinear CBF constraints increase runtime, limiting the horizon size; with a horizon of 5, CasADi solvers drop below 5Hz. Additionally, MPC-CBF often fails to find globally optimal solutions, returning infeasible across all trials. As reported in the table II, MPC-CBF results in large average angular speeds and input tracking errors. Biased MPPI [43] results in local minima at the concave obstacle region preventing the robot from finding a way out. Among the layered baselines, we find that MPC with CBF-QP outperforms MPC with MCBF-QP resulting in lower input errors and lower average $\bar{\omega}$. However, neither approaches escape the concave obstacle region to reach the goal. Through the careful design of a nominal feedback law as in (13), our proposed ADMM-MCBF-LCA successfully navigates the robot out of the concave obstacle to the goal. In supplementary videos ², we show real-robot experiments of our approach outperforming all baselines in indoor environments with static and dynamic obstacles.

VI. CONCLUSION

We conclude that addressing the combined challenges of input feasibility, safety, and real-time computation for robot navigation in environments with moving obstacles, requires layered solutions for robustness and task performance. Our proposed ADMM-MCBF-LCA generated a library of feasible paths offline, to construct a nominal feedback law that is easy to track for our MCBF filter to ensure safety. We demonstrated experiments on realistic Gazebo simulations and hardware showing our approach outperforming baselines in terms of reaching the goal while generating safe and

²https://www.youtube.com/watch?v=YhL_OHK8AZ8

feasible inputs. The baselines representing prior work on reactive methods, and end-to-end solvers perform worse than all layered approaches. We also observed that due to the computation-performance tradeoffs, nonlinear MPC based LCAs do not reach the goal and are stuck in local minima. In future work, we plan to address the question of ADMM convergence rigorously for nonlinear systems.

REFERENCES

- [1] J. Canny, *The complexity of robot motion planning*. MIT press, 1988.
- [2] N. Matni, A. D. Ames, and J. C. Doyle, "Towards a theory of control architecture: A quantitative framework for layered multi-rate control," *arXiv preprint arXiv:2401.15185*, 2024.
- [3] U. Rosolia and A. D. Ames, "Multi-rate control design leveraging control barrier functions and model predictive control policies," *IEEE Control Systems Letters*, vol. 5, no. 3, pp. 1007–1012, 2020.
- [4] R. Grandia, A. J. Taylor, A. D. Ames, and M. Hutter, "Multi-layered safety for legged robots via control barrier functions and model predictive control," in *2021 IEEE International Conference on Robotics and Automation (ICRA)*. IEEE, 2021, pp. 8352–8358.
- [5] U. Rosolia, A. Singletary, and A. D. Ames, "Unified multirate control: From low-level actuation to high-level planning," *IEEE Transactions on Automatic Control*, vol. 67, no. 12, pp. 6627–6640, 2022.
- [6] M. Stolle and C. G. Atkeson, "Policies based on trajectory libraries," in *Proceedings 2006 IEEE International Conference on Robotics and Automation, 2006. ICRA 2006*. IEEE, 2006, pp. 3344–3349.
- [7] A. Majumdar and R. Tedrake, "Funnel libraries for real-time robust feedback motion planning," *The International Journal of Robotics Research*, vol. 36, no. 8, pp. 947–982, 2017.
- [8] K.-C. Hsu, H. Hu, and J. F. Fisac, "The safety filter: A unified view of safety-critical control in autonomous systems," *Annual Review of Control, Robotics, and Autonomous Systems*, vol. 7, 2023.
- [9] J. Borenstein and Y. Koren, "Real-time obstacle avoidance for fast mobile robots," *IEEE Transactions on systems, Man, and Cybernetics*, vol. 19, no. 5, pp. 1179–1187, 1989.
- [10] S. G. Loizou, H. G. Tanner, V. Kumar, and K. J. Kyriakopoulos, "Closed loop motion planning and control for mobile robots in uncertain environments," in *42nd IEEE International Conference on Decision and Control (IEEE Cat. No. 03CH37475)*, vol. 3. IEEE, 2003, pp. 2926–2931.
- [11] S. G. Loizou and V. Kumar, "Mixed initiative control of autonomous vehicles," in *Proceedings 2007 IEEE International Conference on Robotics and Automation*. IEEE, 2007, pp. 1431–1436.
- [12] L. Huber, A. Billard, and J.-J. Slotine, "Avoidance of convex and concave obstacles with convergence ensured through contraction," *IEEE Robotics and Automation Letters*, vol. 4, no. 2, pp. 1462–1469, 2019.
- [13] A. Billard, S. Mirrazavi, and N. Figueroa, *Learning for Adaptive and Reactive Robot Control: A Dynamical Systems Approach*. The MIT Press, 2022.
- [14] A. D. Ames, S. Coogan, M. Egerstedt, G. Notomista, K. Sreenath, and P. Tabuada, "Control barrier functions: Theory and applications," in *2019 18th European control conference (ECC)*. IEEE, 2019, pp. 3420–3431.
- [15] G. Notomista and M. Saveriano, "Safety of dynamical systems with multiple non-convex unsafe sets using control barrier functions," *IEEE Control Systems Letters*, vol. 6, pp. 1136–1141, 2021.
- [16] A. Singletary, K. Klingebiel, J. Bourne, A. Browning, P. Tokumaru, and A. Ames, "Comparative analysis of control barrier functions and artificial potential fields for obstacle avoidance," in *2021 IEEE/RSJ International Conference on Intelligent Robots and Systems (IROS)*. IEEE, 2021, pp. 8129–8136.
- [17] A. Dahlin and Y. Karayiannidis, "Creating star worlds: Reshaping the robot workspace for online motion planning," *Trans. Rob.*, vol. 39, no. 5, p. 3655–3670, jun 2023. [Online]. Available: <https://doi.org/10.1109/TRO.2023.3279029>
- [18] S. M. LaValle, *Planning Algorithms*. USA: Cambridge University Press, 2006.
- [19] Y. Xue and N. Figueroa, "No minima, no collisions: Combining modulation and control barrier function strategies for feasible dynamical collision avoidance," 2025. [Online]. Available: <https://arxiv.org/abs/2502.14238>
- [20] C. K. Fourie, N. Figueroa, and J. A. Shah, "On-manifold strategies for reactive dynamical system modulation with nonconvex obstacles," *IEEE Transactions on Robotics*, vol. 40, pp. 2390–2409, 2024.
- [21] R. M. Murray *et al.*, "Optimization-based control," *California Institute of Technology, CA*, pp. 111–128, 2009.
- [22] E. Todorov and W. Li, "A generalized iterative lqg method for locally-optimal feedback control of constrained nonlinear stochastic systems," in *Proceedings of the 2005, American Control Conference, 2005. IEEE*, 2005, pp. 300–306.
- [23] A. Srikanthan, V. Kumar, and N. Matni, "Augmented lagrangian methods as layered control architectures," *arXiv preprint arXiv:2311.06404*, 2023.
- [24] J. Zeng, B. Zhang, and K. Sreenath, "Safety-critical model predictive control with discrete-time control barrier function," in *2021 American Control Conference (ACC)*. IEEE, 2021, pp. 3882–3889.
- [25] Y. Emam, P. Glotfelter, S. Wilson, G. Notomista, and M. Egerstedt, "Data-driven robust barrier functions for safe, long-term operation," *IEEE Transactions on Robotics*, vol. 38, no. 3, pp. 1671–1685, 2022.
- [26] A. Singletary, S. Kolathaya, and A. D. Ames, "Safety-critical kinematic control of robotic systems," *IEEE Control Systems Letters*, vol. 6, pp. 139–144, 2022.
- [27] M. Saveriano and D. Lee, "Learning barrier functions for constrained motion planning with dynamical systems," in *2019 IEEE/RSJ International Conference on Intelligent Robots and Systems (IROS)*, 2019, pp. 112–119.
- [28] I. Jang and H. J. Kim, "Safe control for navigation in cluttered space using multiple lyapunov-based control barrier functions," *IEEE Robotics and Automation Letters*, vol. 9, no. 3, pp. 2056–2063, 2024.
- [29] E. Rimon and D. Koditschek, "Exact robot navigation using artificial potential functions," *IEEE Transactions on Robotics and Automation*, vol. 8, no. 5, pp. 501–518, 1992.
- [30] H. J. S. Feder and J.-J. Slotine, "Real-time path planning using harmonic potentials in dynamic environments," in *Proceedings of International Conference on Robotics and Automation*, vol. 1. IEEE, 1997, pp. 874–881.
- [31] S. M. Khansari-Zadeh and A. Billard, "A dynamical system approach to realtime obstacle avoidance," *Autonomous Robots*, vol. 32, pp. 433–454, 2012.
- [32] M. Saveriano and D. Lee, "Distance based dynamical system modulation for reactive avoidance of moving obstacles," in *2014 IEEE International Conference on Robotics and Automation (ICRA)*, 2014, pp. 5618–5623.
- [33] A. Billard, S. Mirrazavi, and N. Figueroa, *Learning for Adaptive and Reactive Robot Control: A Dynamical Systems Approach*. MIT Press, 2022.
- [34] A. Dahlin and Y. Karayiannidis, "Creating star worlds: Reshaping the robot workspace for online motion planning," *IEEE Transactions on Robotics*, vol. 39, no. 5, pp. 3655–3670, 2023.
- [35] F. Blanchini, S. Miani, F. Blanchini, and S. Miani, "Invariant sets," *Set-Theoretic Methods in Control*, pp. 121–191, 2015.
- [36] S. Liu, Y. Mao, and C. A. Belta, "Safety-critical planning and control for dynamic obstacle avoidance using control barrier functions," *arXiv preprint arXiv:2403.19122*, 2024.
- [37] L.-Z. Liao and C. A. Shoemaker, "Convergence in unconstrained discrete-time differential dynamic programming," *IEEE Transactions on Automatic Control*, vol. 36, no. 6, pp. 692–706, 1991.
- [38] H. J. Choi and N. Figueroa, "Towards feasible dynamic grasping: Leveraging gaussian process distance field, se (3) equivariance, and riemannian mixture models," in *2024 IEEE International Conference on Robotics and Automation (ICRA)*. IEEE, 2024, pp. 6455–6461.
- [39] S. Boyd, N. Parikh, E. Chu, B. Peleato, J. Eckstein *et al.*, "Distributed optimization and statistical learning via the alternating direction method of multipliers," *Foundations and Trends® in Machine Learning*, vol. 3, no. 1, pp. 1–122, 2011.
- [40] S. Diamond and S. Boyd, "Cvxpy: A python-embedded modeling language for convex optimization," *The Journal of Machine Learning Research*, vol. 17, no. 1, pp. 2909–2913, 2016.
- [41] J. A. E. Andersson, J. Gillis, G. Horn, J. B. Rawlings, and M. Diehl, "CasADI – A software framework for nonlinear optimization and optimal control," *Mathematical Programming Computation*, vol. 11, no. 1, pp. 1–36, 2019.
- [42] J. Bradbury, R. Frostig, P. Hawkins, M. J. Johnson, C. Leary, D. Maclaurin, and S. Wanderman-Milne, "JAX: composable transformations of Python+NumPy programs," 2018. [Online]. Available: <http://github.com/google/jax>

- [43] E. Trevisan and J. Alonso-Mora, "Biased-mppi: Informing sampling-based model predictive control by fusing ancillary controllers," *IEEE Robotics and Automation Letters*, vol. 9, no. 6, pp. 5871–5878, 2024.
- [44] A. D. Ames, X. Xu, J. W. Grizzle, and P. Tabuada, "Control barrier function based quadratic programs for safety critical systems," *IEEE Transactions on Automatic Control*, vol. 62, no. 8, pp. 3861–3876, 2017.
- [45] X. Xu, T. Waters, D. Pickem, P. Glotfelter, M. Egerstedt, P. Tabuada, J. W. Grizzle, and A. D. Ames, "Realizing simultaneous lane keeping and adaptive speed regulation on accessible mobile robot testbeds," in *2017 IEEE conference on control technology and applications (CCTA)*. IEEE, 2017, pp. 1769–1775.